**Supporting Information (SI)**

# Electronic Effect of the Substituents on the Charge Transfer Dynamics at $CsPbBr_3$ Perovskite-Small Molecule Interface

*Soumi Roy, Malay Krishna Mahato, Edamana Prasad* [a*]

a. *Department of Chemistry, Indian Institute of Technology Madras (IITM), Chennai 600036, India.*

| Contents | Page |
|---|---|

- **EXPERIMENTAL SECTION**

**Chemicals.** Cesium carbonate ($Cs_2CO_3$, 99.95%, Sigma-Aldrich), lead bromide ($PbBr_2$, 99.999%, Sigma-Aldrich), oleic acid (OA, 90%, Sigma-Aldrich), 1-octadecene (ODE, 90%, Sigma-Aldrich), n-oleylamine (OLA, 70%, Sigma-Aldrich), chloranilic acid (CA, 2,5-dichloro-3,6-dihydroxy-p-benzoquinone,>98%, Alfa Aesar), para-benzoquinone (BQ,>96%, Sigma-Aldrich), duroquinone (DQ, tetramethyl-p-benzoquinone, 96%, Sigma-Aldrich), were used as purchased without further treatment.

**Structural Characterisation.** Transmission electron microscopy (TEM) measurement. TEM image was obtained using JEOL-3010, 300 kV instrument equipped with Gatan 794 multi scan CCD camera. The accelerating voltage was kept low to minimise beam-induced damage in the sample.

Powder X-ray diffraction (PXRD) measurement. Diffraction pattern of $CsPbBr_3$ NCs were recorded in thin film mode drop casted on cover glass on Bruker AXS D8 diffractometer using Cu Kα radiation (λ=1.54178 A$^o$).

**Optical Characterisation.** Steady state measurements and time-resolved PL experiment. Steady state absorption and emission spectra of $CsPbBr_3$ NCs dispersed in toluene were measured using a JASCO V-760 spectrophotometer and a FluoroMax-4 (HORIBA Jobin Yvon) equipment, respectively. PL decay profiles were recorded in a HORIBA Jobin Yvon Fluorocube equipment in a time-correlated single photon counting (TCSPC) arrangement. A 450 nm LED with 1 MHz pulse repetition rate was the excitation source throughout the experiment. Emission of the samples were collected at 509 nm. The decay curves were analysed using IBH software (DAS6) and the decay profiles were fitted in tri-exponential decay according to equation S1, where $\tau_i$ is the PL lifetime and $a_i$ is the corresponding amplitude of the decay.

$$I(t) = \sum_{i=1}^{3} A_i exp(-t/\tau_i) \qquad \text{(S1)}$$

The average lifetime of fluorescence (amplitude-weighted) was calculated from the following equation (eq S2)

$$\tau_{av} = \frac{\sum_{i=1}^{3} A_i \tau_i}{\sum_{i=1}^{3} A_i} \qquad \text{(S2)}$$

Transient absorption experiment. The transient absorption experiment was done in a femtosecond pump-probe set up (Helios Fire). The seed laser pulse was generated in mode-locked Ti:sapphire laser system (Vitara, coherent) centered at 800 nm with 80 MHz repetition rate and < 110 fs pulse width, and power of 400 nJ. A part (25%) of this beam was amplified by a Ti:sapphire regenerative amplifier (Astrella, coherent) to a amplified beam of 800 nm with an energy of 6 mJ, pulse width of 35 fs and repetation rate of 1kHz. The amplified laser output of 800 nm was split into two parts in 3:1 ratio. The higher energy part of the beam was directed to an optical parametric amplifier (OPA) to generate required excitation (pump) pulse which was 350 nm for this work. The other part of the amplified beam was focused on a 2 mm-thick sapphire plate to produce a white light continuum (WLC), wavelength ranging from 350 nm to 1000 nm, probe pulse. The sample chamber is a 2 mm optical path quartz cylindrical cell set on a variable speed rotating holder. Both the beams were focused into a 100 μm optical fibre equipped with an imaging spectrometer, after passing through the sample. The instrument response function (IRF) for this set up was determined to be about 110 fs.

- **Size distribution histogram of $CsPbBr_3$**

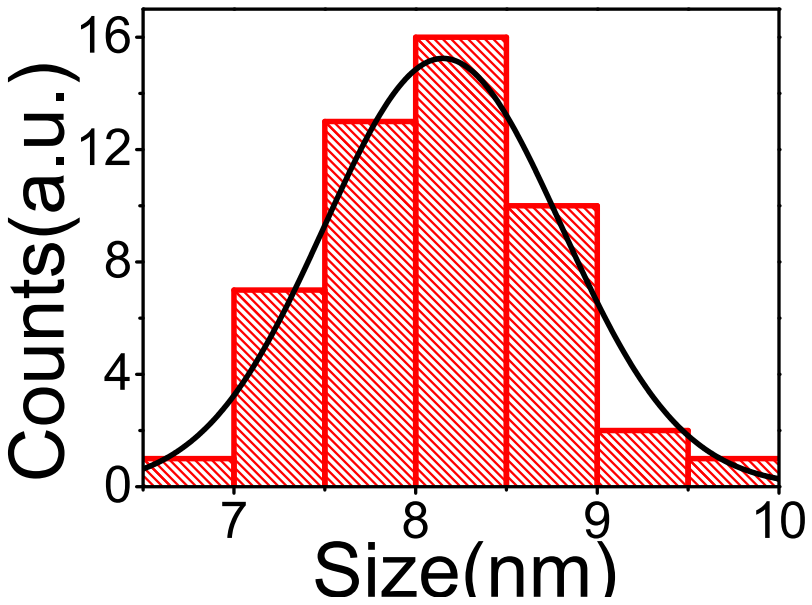


**Figure S1:** Size distribution histogram of the TEM image of $CsPbBr_3$ NCs.

- **Emission spectra of the quencher molecules**

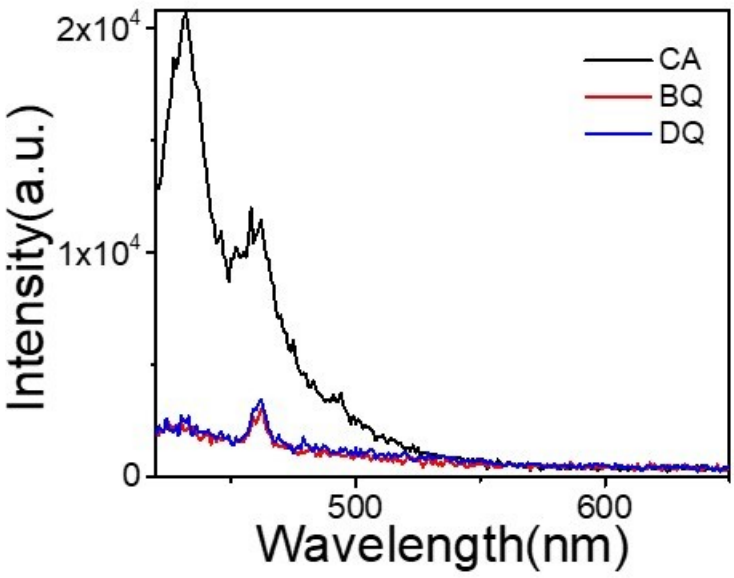


**Figure S2:** Emission ($\lambda_{ex}$=405 nm) spectra of the three quencher molecules after 405 nm excitation.

- **Concentration calculation of the NCs:**

In order to determine the molar concentration of NCs solution, a known weight of dried NCs powder was dispersed in a known volume of toluene. To eliminate the weight contribution of the organic capping ligands from the inorganic $CsPbBr_3$ NCs part, TGA were carried out. TGA shows 11% weight loss due to organic capping ligands. Therefore, 89% of the total weight taken is solely for the inorganic part and was used to calculate the molar concentration (C) of the NCs.(2) Considering cubic shape of the NCs, as revealed by the TEM images, weight of a single NC (m) was calculated using the formula $m = d \times V$, where d is the density of the bulk $CsPbBr_3$ (4.86 g/cc [1] and V is the volume of a single NC ($V=a^3$, a=average edge length of a nano cube obtained from TEM image). The number of NCs present in the solution was obtained by dividing the total weight of the inorganic part of the NCs sample with the weight of a single NC. These numbers of NCs were then converted to number of moles by dividing with Avogadro's number ($N_A$). C of the NCs were then calculated from the knowledge of

the volume of toluene used for dispersing the sample. The concentration of the NCs used for the steady state absorption, emission and time-resolved PL decay study was $2.21\times10^{-8}$ M.

- **Table S1:** PLQY values of $CsPbBr_3$ NC and $CsPbBr_3$ NC- Acceptor composites systems.

| System | PLQY(%) |
|---|---|
| $CsPbBr_3$ | 77±5 |
| $CsPbBr_3$-CA | 30±3 |
| $CsPbBr_3$-BQ | 45±2 |
| $CsPbBr_3$-DQ | 58±3 |

- **Time resolved PL decay titration**

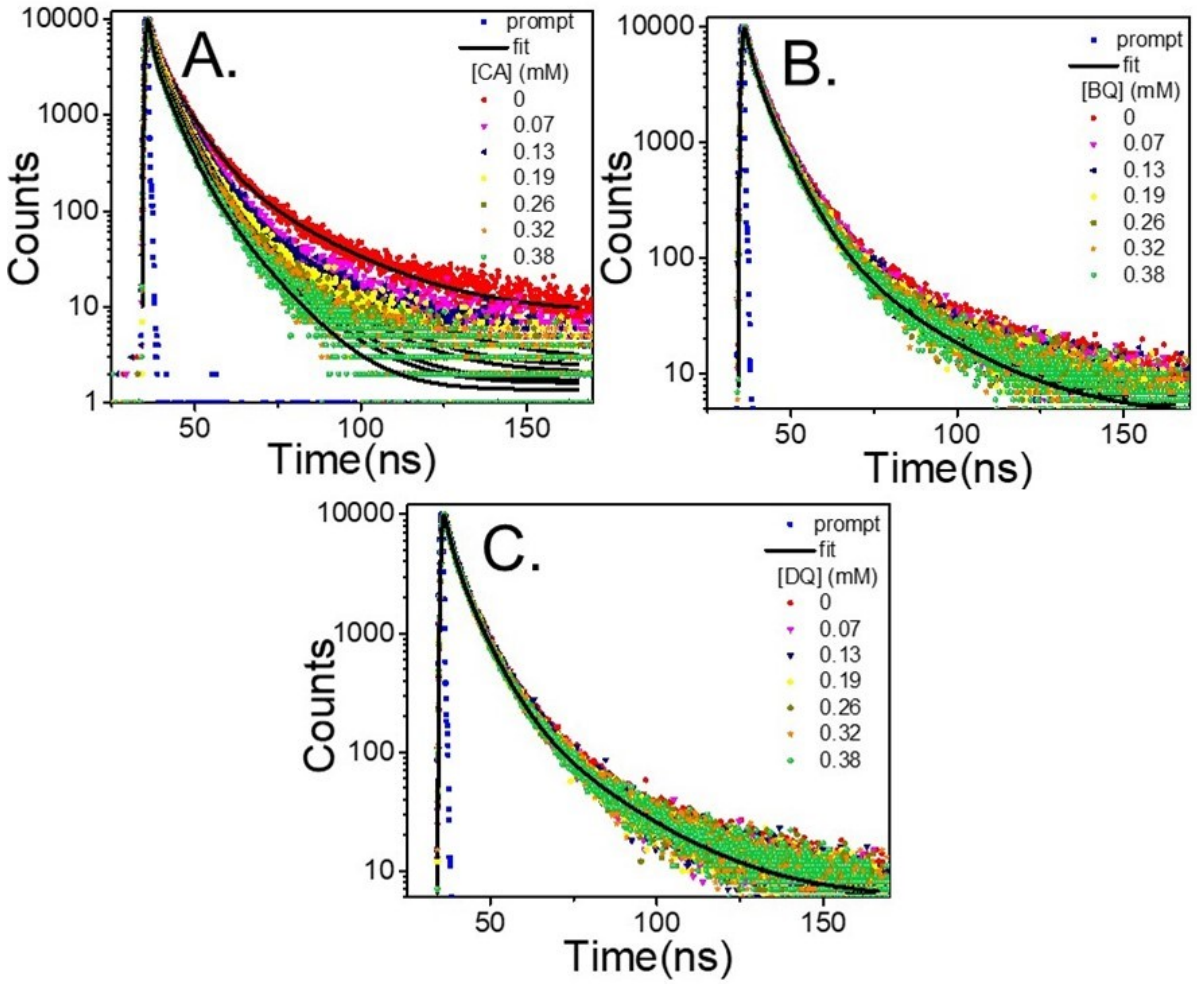


**Figure S3:** Time resolved PL decay quenching titrations of $CsPbBr_3$ NCs against the three individual quenchers.

- **Time resolved PL decay parameters**

**Table S2:** Photoluminescence lifetime decay parameters of $CsPbBr_3$ NCs in presence of different acceptors with increasing concentration.

| Quencher | Concentration (mM) | $A_1$[a] % | $\tau_1$[b] ns | $A_2$[a] % | $\tau_2$[b] ns | $A_3$[a] % | $\tau_3$[b] ns | $\tau_{avg}$ ns |
|---|---|---|---|---|---|---|---|---|
| CA | 0 | 26 | 2.19 | 62 | 7.43 | 12 | 31.08 | 8.91±0.11 |
| | 0.066 | 28 | 1.57 | 59 | 5.92 | 13 | 20.78 | 6.63±0.15 |
| | 0.1315 | 29 | 1.37 | 59 | 5.26 | 12 | 15.23 | 5.33±0.20 |
| | 0.1960 | 31 | 1.34 | 58 | 5.12 | 11 | 14.79 | 5.01±0.12 |
| | 0.2597 | 32 | 1.05 | 58 | 4.82 | 10 | 14.42 | 5.57±0.18 |
| | 0.3225 | 33 | 0.88 | 57 | 4.49 | 10 | 14.18 | 4.27±0.22 |
| | 0.3846 | 34 | 0.61 | 56 | 3.85 | 10 | 13.55 | 3.72±0.11 |
| BQ | 0 | 26 | 2.15 | 62 | 7.49 | 12 | 29.98 | 8.80±0.11 |
| | 0.066 | 27 | 2.22 | 61 | 6.94 | 12 | 25.88 | 7.94±0.22 |
| | 0.1315 | 28 | 1.83 | 60 | 6.30 | 12 | 22.98 | 7.05±0.25 |
| | 0.1960 | 29 | 1.75 | 60 | 6.08 | 11 | 21.38 | 6.51±0.14 |
| | 0.2597 | 29 | 1.62 | 60 | 5.88 | 11 | 20.12 | 6.21±0.12 |
| | 0.3225 | 30 | 1.46 | 59 | 5.50 | 11 | 19.55 | 5.83±0.15 |
| | 0.3846 | 31 | 1.32 | 59 | 5.29 | 10 | 18.81 | 5.41±0.18 |
| DQ | 0 | 26 | 2.11 | 62 | 7.38 | 12 | 31.12 | 8.86±0.11 |
| | 0.066 | 27 | 1.98 | 61 | 7.10 | 12 | 29.93 | 8.46±0.15 |
| | 0.1315 | 28 | 1.82 | 60 | 6.88 | 12 | 29.11 | 8.13±0.20 |
| | 0.1960 | 29 | 1.69 | 59 | 6.57 | 12 | 28.77 | 7.82±0.14 |
| | 0.2597 | 29 | 1.52 | 59 | 6.19 | 12 | 27.72 | 7.42±0.13 |
| | 0.3225 | 30 | 1.37 | 59 | 5.98 | 11 | 26.52 | 6.86±0.22 |
| | 0.3846 | 30 | 1.26 | 58 | 5.75 | 12 | 25.95 | 6.83±0.17 |

[a] = ±1%, [b] = 0.10 ns

- **FTIR spectra**

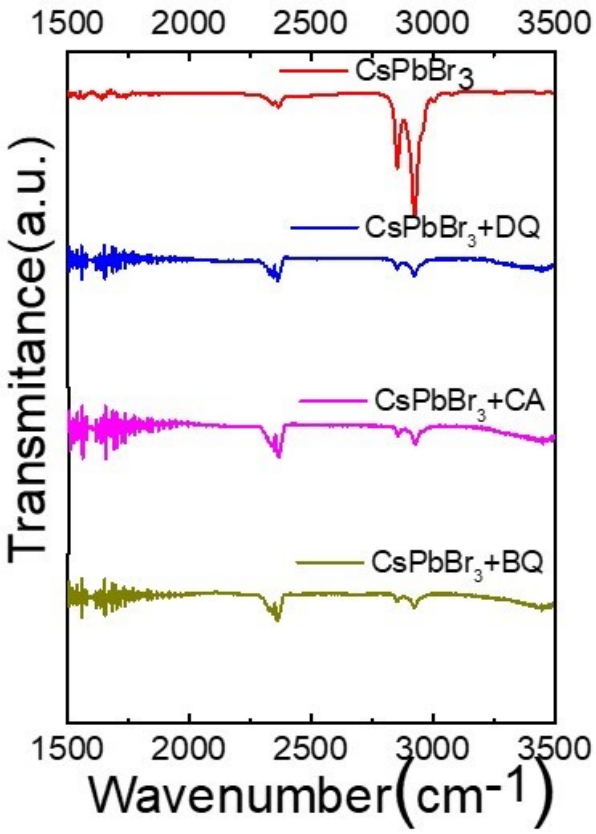


**Figure S4:** FTIR spectra of pristine $CsPbBr_3$ NCs and NC-acceptor composites.

- **TEM image of NC-acceptor composite**

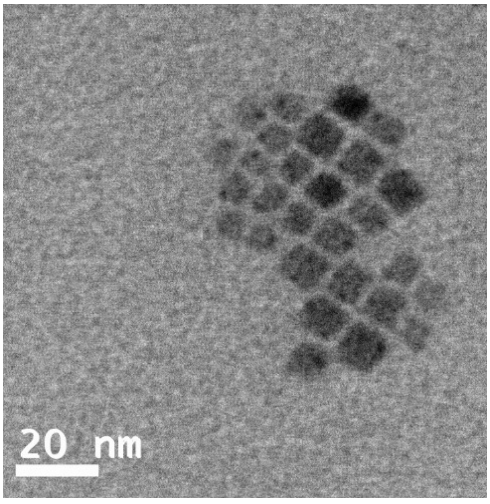


**Figure S5:** TEM image of $CsPbBr_3$-CA composite.

- **$K_{SV}s$ from steady state and time resolved quenching**

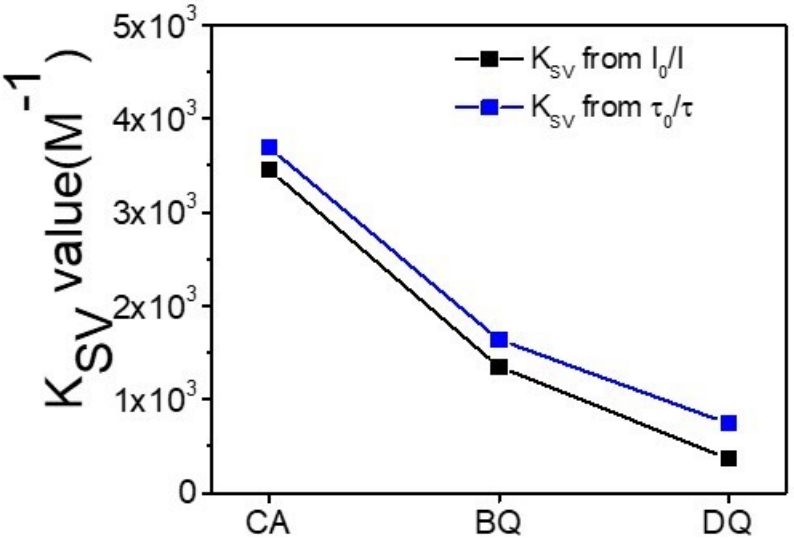


**Figure S6:** Stern-Volmer quenching constants obtained from steady state and time resolved PL quenching.

- **Overlap spectra**

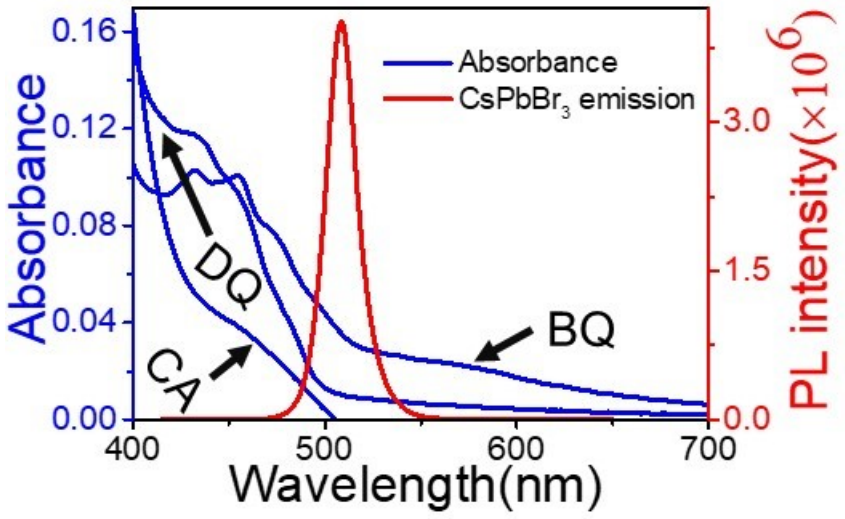


**Figure S7:** Overlap between absorption spectra of the quenchers and emission spectra of the NCs.

- **Absorbance of the quencher molecules with respect to the NCs**

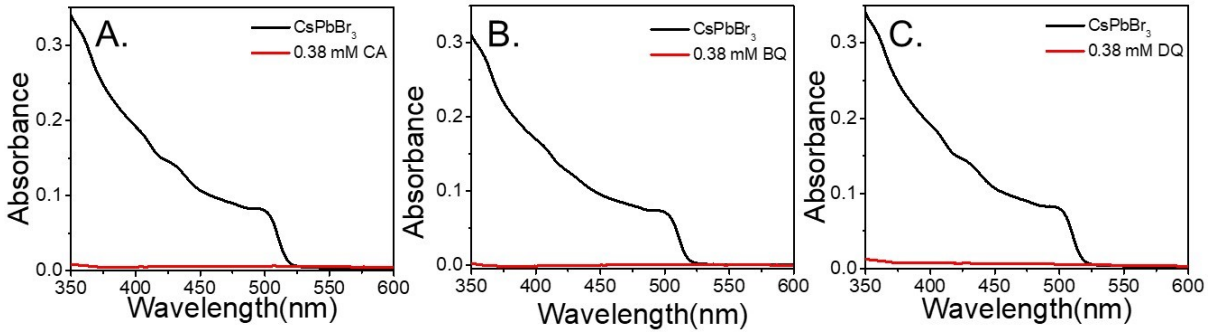


**Figure S8:** Steady state absorbance of A. CA B. BQ and C. DQ with respect to $CsPbBr_3$ NCs.

- **TA spectra**

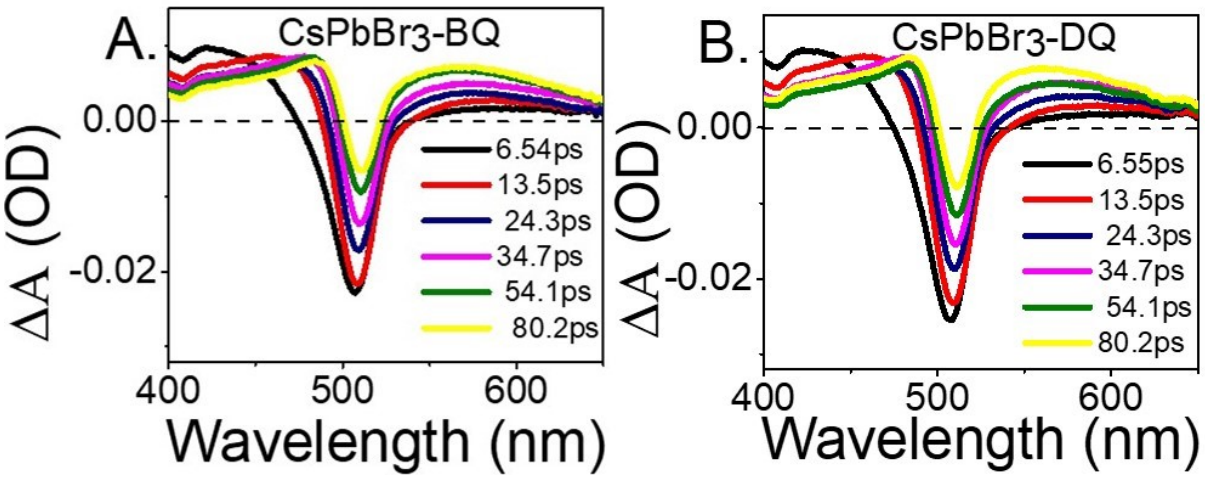


**Figure S9:** TA spectra of A. $CsPbBr_3$-BQ, B. $CsPbBr_3$-DQ composite systems at different delay times after 350 nm excitation.

- **Computational details:**

Geometry optimisation of the quencher molecules in the ground state was done using B3LYP/6-31(+) G(d) level of theory.

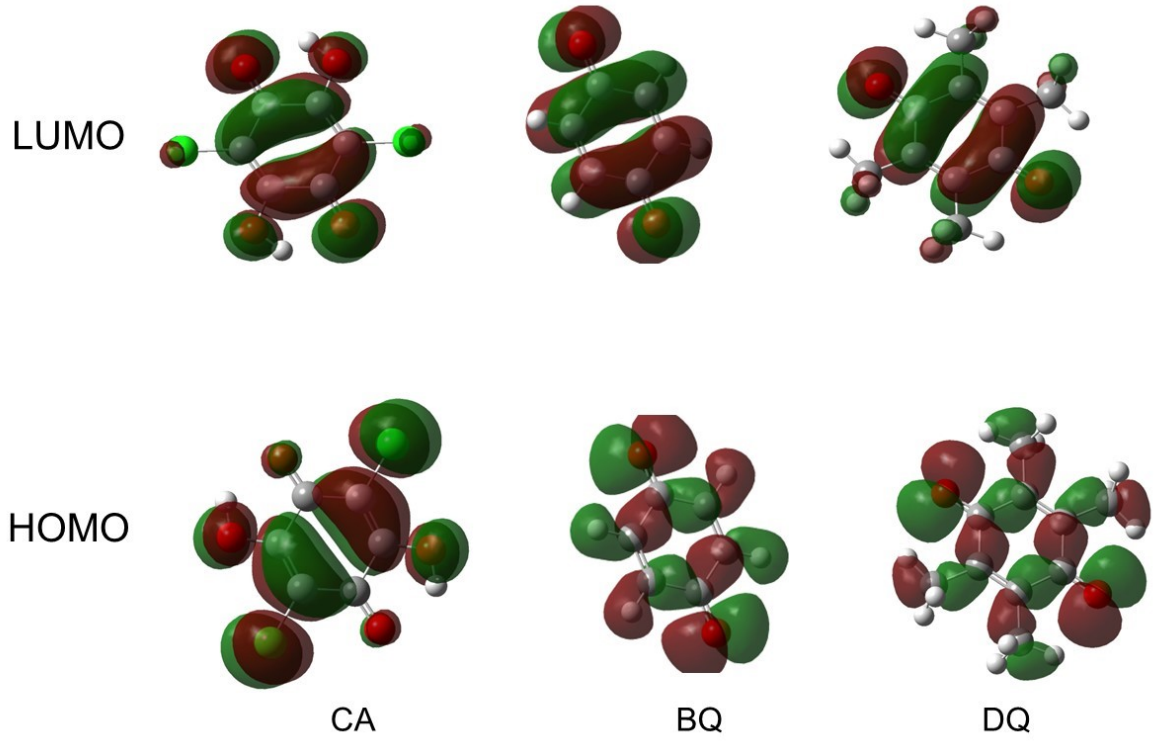


**Figure S6:** HOMO and LUMO molecular orbitals of the three quenchers.

- **Tauc plot**

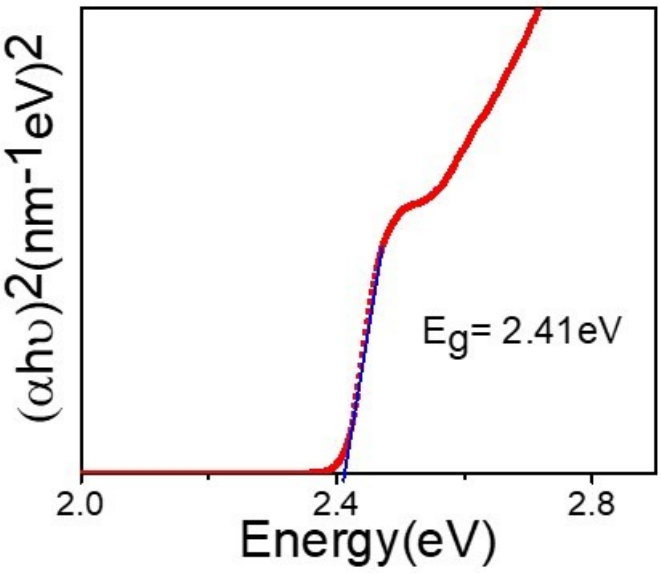


**Figure S10:** Tauc plot for band gap ($E_g$) calculation of $CsPbBr_3$ NCs.

- **Calculation of rate of electron transfer ($k_{ET}$):**

Rate of electron transfer ($k_{ET}$) from the $CsPbBr_3$ NCs had been calculated before using Marcus theory.[2] The functional form of Marcus model is given below:

$$k_{ET} = \frac{4\pi^2}{h}|H(E)|^2\frac{1}{\sqrt{4\pi\lambda k_B T}}exp[-\frac{(\lambda+\Delta G)^2}{4\lambda k_B T}] \quad \text{(S3)}$$

where $k_{ET}$ is the rate of charge transfer, h is the Planck's constant, $H$ ($E$) stands for overlap matrix element, $k_B$ is the Boltzmann's constant, T is temperature, λ is the system reorganisation energy, $\Delta G$ is the free energy change between the donor and acceptor systems. H(E) represents the overlap between the donating and accepting state wavefunctions. Theoretical models to evaluate this term had been used previously to describe coupling between all organic donor–acceptor pairs.[3] Since organic molecules have discrete energy levels, hence this overlap integral

appears to be as small as ~5 $cm^{-1}$. [4] In case of metal oxide nanoparticle acceptors, as they have quasi continuous energy levels, the values of H(E) were reported to be 100 and 350 $cm^{-1}$ for $TiO_2$ and $SnO_2$ nanoparticles, respectively.[5] But in our case, the donor is a nanocrystal with quasi continuous energy levels and the acceptors are small organic molecules. Due to lack of theoretical models and experimental evidences, we approximately took H(E) equals to 5 $cm^{-1}$. ΔG was calculated using the following equation,[6]

$$\Delta G = E_{acceptor} - E_{NC} + \frac{e^2}{2R_{NC}} + \frac{2.2e^2}{\varepsilon_{NC}R_{NC}} - \frac{e^2\,(\varepsilon_{acceptor} - 1)}{4(R_{NC} + l)\,(\varepsilon_{acceptor} + 1)} \quad \text{(S2)}$$

where $E_{acceptor}$ is the LUMO potential of the acceptor which we calculated from DFT study. $E_{NC}$ is the conduction band minimum (CBM) energy of the NCs. $e$ is the elementary charge, $R_{NC}$ and $\varepsilon_{NC}$ are radius and dielectric constant of the NCs, $l$ is NC-acceptor separation distance. $l$ was taken to be 0 nm because the distance between NCs and acceptors are negligible compared to NCs size. $\varepsilon_{acceptor}$ is the dielectric constant of the acceptor which we approximated as 2.41 (dielectric constant of toluene) as the acceptor concentration is very less in the medium. $\varepsilon_{NC}$ was taken as 4.631 according to literature.[7] With all these parameters, we calculated ΔG of electron transfer to be ~ 1.06 eV, 0.72 eV and 0.17 eV for CA, BQ and DQ, respectively. Now, to calculate the rate we are only left with the parameter λ, system reorganisation energy. This reorganisation energy includes two terms; energy change due to variation of electronic energy levels due to geometry changes of the reactants (internal reorganisation energy) and the energy change due to solvent molecules reorganisation during the charge transfer process. Internal reorganisation energy for electron transfer from $CsPbI_3$ had been reported to be 1.642 eV.[8,9] Since, the electronic structures of valance and conduction bands and the density of electronic states are identical in these $CsPbX_3$ (X=Cl, Br, I) compounds,[6] we approximately took λ=1.642 eV for our $CsPbBr_3$ system as well. Solvent reorganisation energy we have neglected, since it would be very less for a non-polar toluene medium. With all these approximations, we

calculated the rate constants ($k_{ET}$) are $6.76\times10^{8}$ $s^{-1}$, $3.25\times10^{7}$ $s^{-1}$, $1.32\times10^{4}$ $s^{-1}$ for CA, BQ and DQ, respectively.

- **Growth kinetics**

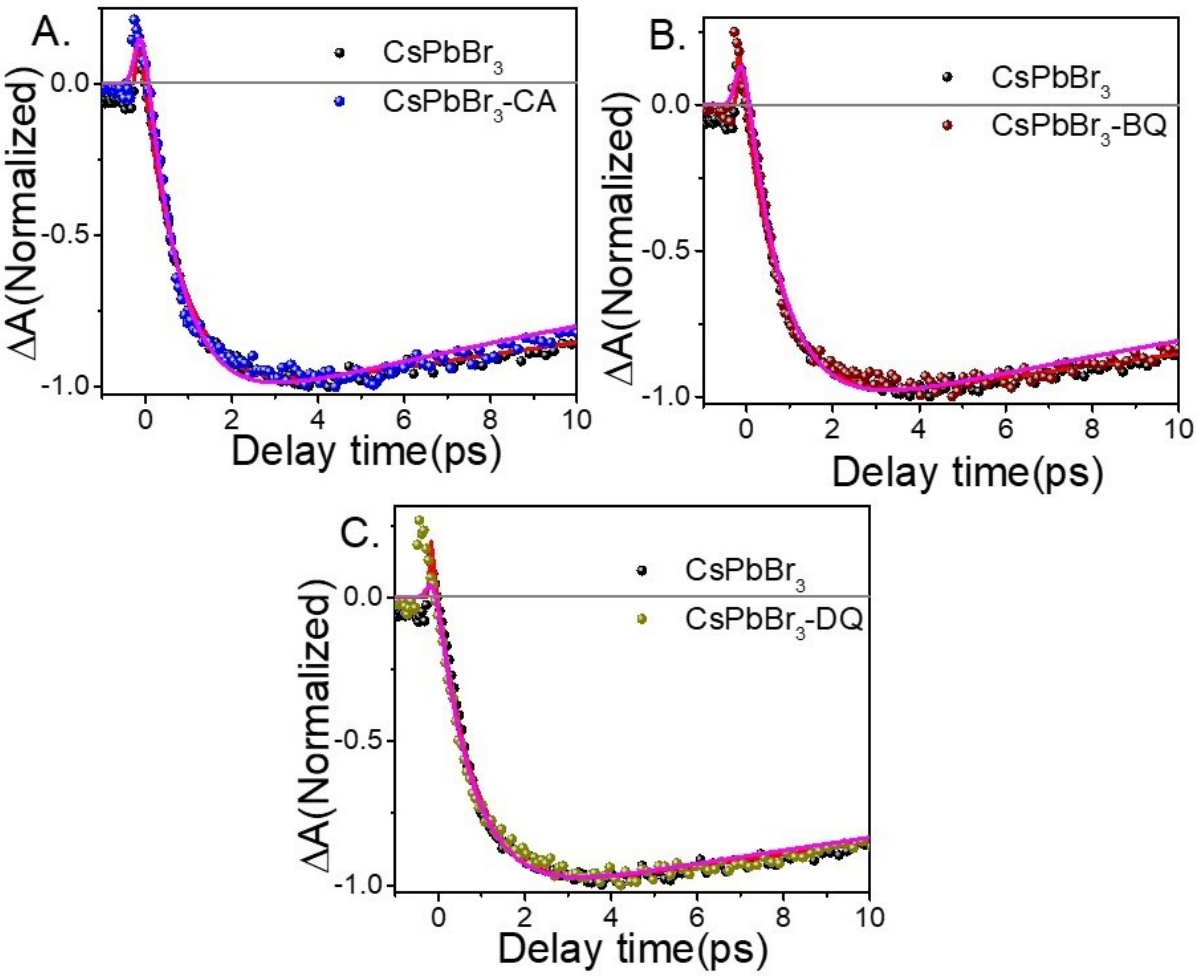


**Figure S11:** Growth kinetics of the three NC-acceptor composite systems with respect to bare NCs at 505 nm.

- **$k_{ET}$ vs. ΔG**

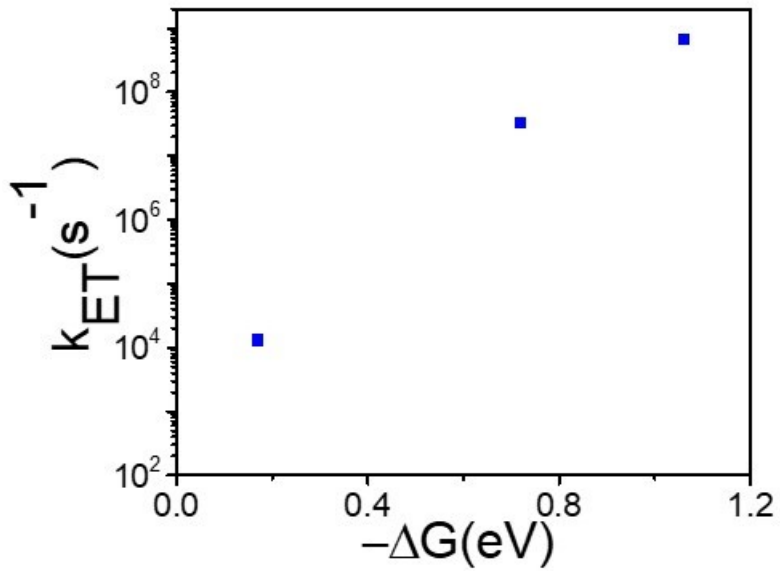


**Figure S12:** Rate constant of electron transfer as a function of the free energy change.

**REFERENCES**

(1) V. K. Ravi, A. Swarnkar, R. Chakraborty, A. Nag, Excellent green but less impressive blue luminescence from $CsPbBr_3$ perovskite nanocubes and nanoplatelets. *Nanotechnology* **2016**, *27*, 325708.

(2) R. A. Marcus. On the Theory of Oxidation-Reduction Reactions Involving Electron Transfer. I. *J. Chem. Phys*. **1956**, *24*, 966-978.

(3) K. Kemnitz, N. Nakashima, K. Yoshihara. Electron Transfer by Isolated Rhodamine B Molecules Adsorbed on Organic Single Crystals. A Solvent-Free Model System. *J. Phys. Chem.* **1988**, *92*, 3915-3925.

(4) E. Prasad, K. R. Gopidas. Photoinduced Electron Transfer in Hydrogen Bonded Donor-Acceptor Systems. Study of the Dependence of Rate on Free Energy and Simultaneous Observation of the Marcus and Rehm-Weller Behaviors. *J. Am. Chem. Soc*. **2000**, *122*, 3191-3196.

(5) C. She, N. A. Anderson, J. Guo, F. Liu, W. H. Goh, D. T. Chen, D. L. Mohler, Z. Q. Tian, J. T. Hupp, T. Lian. pH-dependent electron transfer from re-bipyridyl complexes to metal oxide nanocrystalline thin films. *J Phys Chem B*. **2005**, *109*, 19345–19355.

(6) K. Tvrdy, P. A. Frantsuzov, P. V. Kamat. Photoinduced Electron Transfer from Semiconductor Quantum Dots to Metal Oxide Nanoparticles. *Proc. Natl. Acad. Sci. U.S.A.* **2011**, *108*, 29-34.

(7) G. Murtaza, I. Ahmad. First Principle Study of the Structural and Optoelectronic Properties of Cubic Perovskites $CsPbM_3$ (M= Cl, Br, I). *Phys. B.* **2011**, *406*, 3222-3229.

(8) A. J. Neukirch, W. Nie, J. C. Blancon, K. Appavoo, H. Tsai, M. Y. Sfeir, C. Katan, L. Pedesseau, J. Even, J. J. Crochet, G. Gupta, A. D. Mohite, S. Tretiak. Polaron Stabilization by Cooperative Lattice Distortion and Cation Rotations in Hybrid Perovskite Materials. *Nano Lett.* **2016**, *16*, 3809-3816.

(9) F. Liu, Y. Zhang, C. Ding, T. Toyoda, Y. Ogomi, T. S. Ripolles, S. Hayase, T. Minemoto, K. Yoshino, S. Dai, Q. Shen. Ultrafast Electron Injection from Photoexcited Perovskite $CsPbI_3$ QDs into $TiO_2$ Nanoparticles with Injection Efficiency near 99%. *J. Phys. Chem. Lett.* **2018**, *9*, 294−29.